Extended Abstracts of the 2014 International Conference on Solid State Devices and Materials, Tsukuba, 2014, pp532-533

Metal-induced crystallization of amorphous Ge on insulators: Comparative study of catalytic effects between Al and Sn

N. Oya, K. Toko, and T. Suemasu

Institute of Applied Physics, University of Tsukuba, Tsukuba, Ibaraki 305-8573, Japan
Phone: +81-29-853-5472, Fax: +81-29-853-5205, E-mail: bk201011008@s.bk.tsukuba.ac.jp

1. Introduction

An expensive bulk Ge wafer has been used in the bottom cell of high-efficiency tandem solar cells. If the Ge wafer is substituted with a Ge film on an inexpensive glass substrate, the fabrication cost of the tandem solar cell will be reduced [1]. However, thin (<1 μm) Ge films cannot absorb near-infrared lights sufficiently because of its indirect transition at 0.66 eV. GeSn alloy is one of the possible solutions to this because GeSn with high Sn contents (>10%) provides the indirect-to-direct transition [2].

This paper investigates a way to form polycrystalline GeSn thin films on insulators. First, we introduce Al-induced crystallization (AIC) enabling large-grained, orientation-controlled polycrystalline Ge (poly-Ge) thin films on insulators [3]. Utilizing the concept of AIC, we attempt to form high Sn-content GeSn thin films on insulators at low temperatures.

2. Experimental Procedures

We prepared two samples in this study: amorphous Ge (a-Ge) layers were crystallized by using catalytic effects of Al (sample A) and Sn (sample B). For sample A, the Al and a-Ge layers (50-nm thickness each) were prepared in sequence on SiO_2 glass substrates. Between the Al and Ge deposition cycles, the Al layers were exposed to air for 5 min to form native AlO_x membranes, working as a diffusion limiting layer. In the AIC process, the a-Ge layer on Al is crystallized by exchanges between the Al and Ge layers during annealing at 325 °C for 100 h in N_2 ambient, as schematically shown in Fig. 1. For sample B, the a-Ge and Sn layers (100-nm thickness each) were prepared in sequence on SiO_2 glass substrates, and then annealed at 70–250 °C in N_2 ambient. All depositions were carried out at room temperature using a radio-frequency magnetron sputtering method. After the completion of crystallization, metal layers were removed by using diluted HF (1.5%) etching to bare poly-Ge layers.

3. Results and Discussion

For sample A after annealing, the completion of layer exchange was confirmed by using Nomarski optical microscopy. Electron backscattering diffraction (EBSD) measurement revealed that the resulting poly-Ge layer is highly (111)-oriented in z direction as shown in Fig. 2(a). This (111) orientation is explained from the perspective to the minimization of the interface energy between Ge and SiO_2. Moreover, Fig. 2(b) indicates large grains, attributed to the AlO_x interlayer limiting Ge nucleation. The area fraction of (111) orientation was found to be 99%, and the average grain size was found to be over 100 μm by using EBSD analysis.

The cross-section crystal structure of the AIC-Ge film was observed by transmission electron microscopy (TEM). A bright-field TEM image and energy dispersive X-ray (EDX) analysis proved the layer exchange of Ge and Al layers and the uniform formation of the Ge layer on the SiO_2 substrate. A dark-filed TEM image in Fig. 3 shows the uniform bright contrast of the Ge layer, indicating a single-crystal Ge containing no grain boundaries or stacking faults.

In contrast, for sample B, we could not confirm layer exchange between the Ge and Sn layers. This difference between Al and Sn is likely attributed to the difference of their solubility limits and/or diffusion coefficients to Ge: Sn diffuses into Ge for sample B while Ge diffuses into Al for sample A. However, the Sn catalyst enabled the significant low-temperature crystallization of a-Ge, shown as follows.

The Raman spectra of sample B after annealing at 70 °C are shown in Fig. 4. With increasing annealing time, a Raman peak at around 300 cm^{-1}, originated from Ge-Ge vibration mode, is more clearly observed. Moreover, the left shift from the actual Ge-Ge peak (300 cm^{-1}) is observed, indicating the formation of GeSn containing substitutional Sn atoms. The peak intensity of sample B annealed for 100 h is equal to that for 150 h, suggesting the growth completion of GeSn within 100 h at temperatures as low as 70 °C. This annealing temperature is the lowest value reported so far for crystallizing a-Ge.

The annealing temperature dependence of the Raman spectra for sample B was evaluated, and shown in Fig. 5. The higher the annealing temperature, the sooner the growth of GeSn was completed. Note that the Raman peak shift from 300 cm^{-1} becomes more pronounced at lower annealing temperatures, as summarized in the left axis of Fig. 6. This is consistent with previous reports on the molecular beam epitaxy of GeSn: low temperature growth yields high Sn-content GeSn because of inducing the non-equilibrium condition during growth [4]. From the peak shifts, we calculated Sn concentration in the resulting

GeSn layer, as shown in the right axis of Fig. 6. The Sn concentration increases at lower temperatures: 70 °C annealed sample enables the Sn concentration of as high as nearly 20%. The direct transition at near-infrared region should be expected. The detailed crystal structure of the resulting GeSn layer is now under investigation.

4. Conclusion

A large-grained, (111)-oriented Ge thin film was demonstrated on glass through layer exchange in AIC. On the other hand, we found that layer exchange using Sn as a catalyst was difficult likely because of the dominant Sn diffusion into Ge; however, the significant low-temperature growth (70 °C) of GeSn was achieved. Raman measurement suggested the high Sn content of nearly 20% in the resulting polycrystalline GeSn films on glass. This achievement opens up the possibility of inexpensive optical devices enabling infrared-light absorption.

Acknowledgements

This work was financially supported by the Japan Science Society and the Iwatani Naoji Foundation. The authors are grateful to Prof. N. Usami of Nagoya University and Dr. N. Fukata of NIMS for assistance in some measurements.

References

[1] M. G. Mauk *et. al.*, J. Cryst. Growth **250** (2003) 50.
[2] V. D'Costa *et. al.*, Phys. Rev. B **73** (2006) 125207.
[3] K. Toko *et. al.*, Appl. Phys. Lett. **101** (2012) 072106.
[4] Y. Shimura *et. al.*, Thin Solid Films **518** (2010) S2-S5.

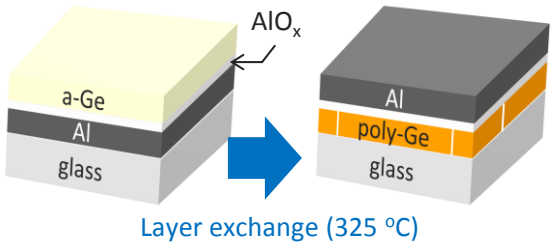

Fig. 1. Schematic of sample A: AIC of an a-Ge thin film on glass.

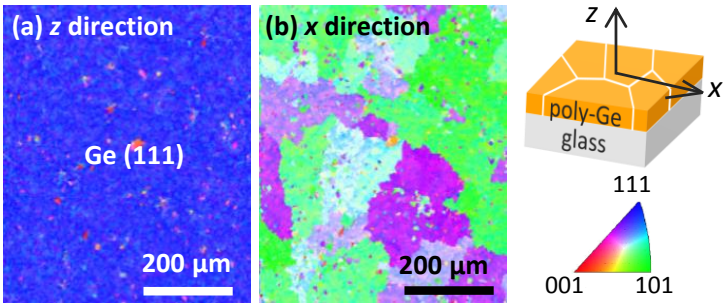

Fig. 2. EBSD images of sample A observed in (a) *z* direction and (b) *x* direction.

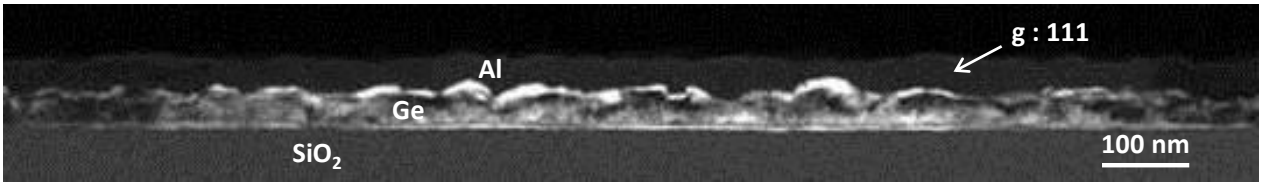

Fig. 3. Cross-sectional dark-field TEM image of sample A, showing a single-crystal Ge.

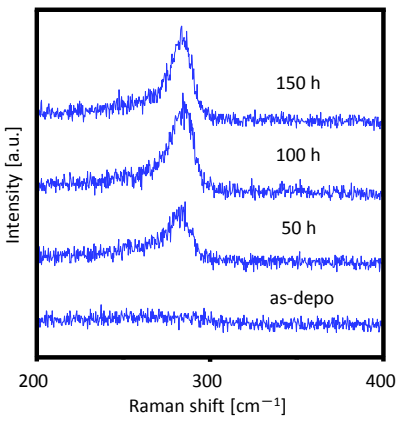

Fig. 4. Raman spectra of sample B before and after annealing at 70 °C for 50-150 h.

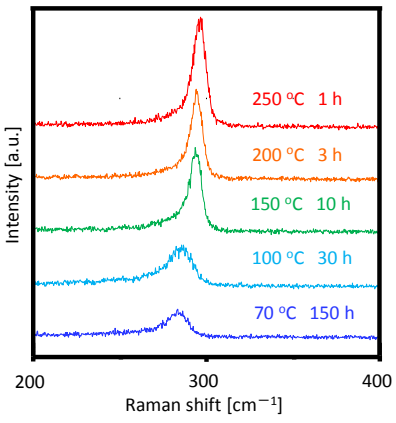

Fig. 5. Raman spectra of sample B after annealing at 70-250 °C.

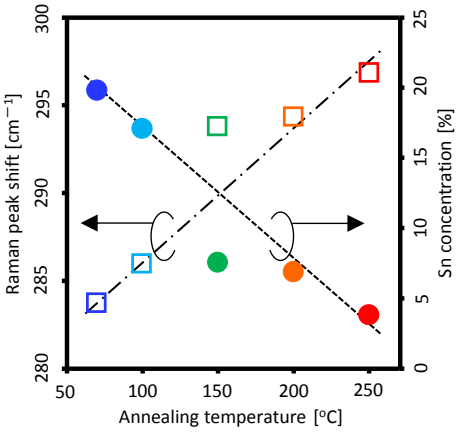

Fig. 6. Annealing temperature dependence of the Raman peak shift and the calculated Sn concentration in sample B.